ACS OMEGA

Open Access

http://pubs.acs.org/journal/acsodf

Article

Effect of Additives on the Morphology of γ-Aminobutyric Acid Crystals

Zhiying Pan, Xiaoyu Cao, Wenyu Ke, Jingyu Wang, Yan Wang,* Shichao Du,* and Fumin Xue*

Cite This: *ACS Omega* 2024, 9, 29928−29938

Read Online

ACCESS | Metrics & More | Article Recommendations | Supporting Information

ABSTRACT: The effect of surfactant, polymer, and tailor-made additives on the crystallization of γ-aminobutyric acid (GABA) was studied in this work. Cooling crystallization of GABA in water yielded plate-like crystals. In the presence of sodium stearate, polyhedral block-like crystals of GABA were obtained. Hydroxyethyl cellulose (HEC) led to rod-like crystals, in which the morphology was associated with additive concentrations. Six kinds of amino acids were used as tailor-made additives, and they exhibit different influences on crystal shape and size. The induction time of GABA was determined in the absence and presence of additives. The results showed that sodium stearate promoted nucleation, while HEC, L-Lysine, L-histidine, and L-tyrosine inhibited nucleation. Crystal face indexing, Hirshfeld surface analysis, and molecular dynamics (MD) simulation in aqueous solution−crystal systems were carried out to investigate the affecting factors of different crystal faces. The polymer additive was selected as an example during MD simulation to calculate intermolecular interactions between the crystal face and solvent or additive. The effect of the additive on the mobility of the solute in solution was also evaluated by mean-square displacement. The additive offers an effective approach for changing crystal morphology and particle size and adapting it to different production requirements.

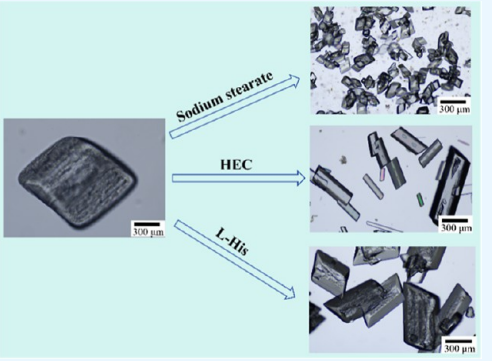

1. INTRODUCTION

Crystallization is an important process in the chemical and pharmaceutical industries.[1] In solution crystallization, the compounds with low purity will be dissolved in the solution, and the difference in solubility allows the compounds with high purity to be crystallized.[2−4] Crystal shape and size are important characteristics affecting the physical and chemical properties of products, and they also play a decisive role in the final performance of the product, including flowability and dissolution rate.[5] Crystal shape is related to the relative growth rate of each crystal face. If the relative growth rate of one crystal face is much faster, the crystal shape tends to be needle.[6] Needle-like crystals have poor flowability but dissolve fast. Hence, the desired shape will change according to different product demand.[7−9] Particles with larger size usually have high bulk density, which is conducive to product packaging.[10] Smaller particles are favored for insoluble drugs because they have faster dissolution rate.[11,12] By controlling the crystal size, sustained or controlled release of the drug can be achieved, and the speed and dose of the drug can be precisely controlled in the body, so that the concentration of the drug is kept stable within the therapeutic range.[13] Therefore, it is of great significance to regulating crystal morphology in the crystallization process.[14]

Crystal shape and size can be changed by the operating conditions, including solvent, supersaturation, seeds, temperatures, and additives. In recent years, the modification of crystal morphology by additives has attracted increasing attention.[15,16] A small number of additives could affect the growth process and change the crystal morphology. Additives can be categorized as ions, molecules, and macromolecules.[17,18] Xie et al. found that polyvinylpyrrolidone (PVP) had a strong inhibitory effect on the growth of salbutamol sulfate crystals. After adding a small amount of PVP K 25 to salbutamol sulfate solution, the crystal habit changed from needle-like to block-like shape.[19] The adsorption of PVP on the crystal surface hindered the diffusion of solute molecules, thus changing the growth rate of the crystal surface. Addadi et al. proposed the concept of tailor-made additives, by which he believed that crystals could be bound on preselected surfaces, thereby inhibiting growth in a predictable manner.[1] Tailor-made additives generally have a similar structure to model substance.[20] Civati et al.[16] found that the addition of additives with similar structure could effectively reduce the aspect ratio of 1:1 eutectic of benzoic acid and isonicotinamide, which inhibited the growth rate of the tip of needle-like crystals. According to Poornachary et al., adding asparagine or glutamic acid into the α-glycine solution could inhibit the growth of α-

Received: May 15, 2024
Revised: June 16, 2024
Accepted: June 18, 2024
Published: June 25, 2024

glycine crystals on the *b*-axis and the *c*-axis.[21] Therefore, crystal morphology can be effectively modified by selecting appropriate additive type and concentration.[22]

γ-Aminobutyric acid (GABA, $C_4H_9NO_2$) is a nonprotein amino acid widely distributed in vertebrates, plants, and microorganisms.[23,24] Following years of research, scientists had discovered that GABA is the main inhibitory neurotransmitter in the mammalian central nervous system and plays a significant role in regulating neuronal excitability.[25] Because of its physiological functions of anticonvulsant, sedation, antihypertensive, and diuretic, GABA has a broad market prospect. At present, the preparation of GABA is mainly done by chemical synthesis and biological transformation. In the separation and purification of GABA, crystallization is a crucial method.[26] Zhao et al. determined the solubility of GABA in a single solvent and a binary mixed solvent, which provided a thermodynamic basis for studying crystallization of GABA.[27] Two anamorphic forms of GABA (form I and form II) were reported by Tomita and Dobson.[24,28] Form I is stable, and form II is metastable. Wang et al. successfully prepared form II by means of additive induction and then identified a new GABA polymorph (form III) by mechanochemical milling.[29] It is worth noting that the stability of the three GABA polymorphisms increases in the order III < II < I at room conditions.[30] However, the crystal morphology of GABA has not yet been studied yet. The study of the crystal morphology of GABA is also of guiding significance for industrial production.

In this work, the crystal morphology of GABA was regulated by cooling crystallization in pure water. The effects of surfactant (sodium stearate), polymer [hydroxyethyl cellulose (HEC)], and tailor-made additives (L-valine, L-leucine, L-isoleucine, L-histidine, L-lysine, and L-tyrosine) on the crystallization of GABA were investigated. The crystal form, morphology, and particle size distribution were analyzed by various solid characterization methods. The induction period in the presence and absence of GABA additives was determined. Molecular simulations were carried out, and intermolecular interactions between the crystal and solvent or additive were calculated to further explore the nucleation and crystal growth behavior of GABA.

2. EXPERIMENTAL SECTION

2.1. Materials and Methods. GABA (purity ≥99.0 wt %), L-valine (L-Val), L-leucine (L-Leu), L-isoleucine (L-Ile), L-histidine (L-His), L-tyrosine (L-Tyr), HEC, and sodium stearate were purchased from Shanghai Aladdin Biochemical Technology Co., and L-lysine(L-Lys) was purchased from Macklin Reagent Co., Ltd. Deionized water was prepared in our laboratory (Arium Advance EDI, Sartorius, Germany). All reagents were used as received. The molecular structures of additives are depicted in Figure S1.

2.2. Cooling Crystallization Experiment. Cooling crystallization of GABA was carried out in water. The experiment was performed in a 200 mL double-jacketed crystallizer equipped with overhead stirring at 200 rpm. The temperature of the GABA solution was controlled by a water circulation bath (Ministat 230, Huber, Berching, Germany). 100 g of GABA solution saturated at 45 °C with and without additives was prepared. The concentration of GABA was calculated based on the solubility data reported by Zhao et al.[27] At 5 °C above the saturation temperature, GABA solids were completely dissolved in the suspension and cooled to a final temperature of 10 °C at a cooling rate of 0.2 °C·min^{-1}. After the suspension was maintained at a final temperature for about 30 min, crystals were filtered and dried. In order to explore the effect of additives (tailor-made additives, polymers, and surfactants) on crystallization of GABA, three different concentrations of each additive were designed (0.005, 0.01, and 0.05% based on the mass of solution). To explore the impact of additives on nucleation, we also determined that the induction time of GABA was also determined. Supersaturated solution was prepared by dissolving a certain amount of GABA in water at a higher temperature and then quickly cooling to 25 °C. The initial supersaturation at 25 °C was set as 1.2. The turbidity of the solution was monitored by a turbidity probe (PHarmaVision Nanosonic Technology Ltd., China). The nucleation time of GABA in the absence and presence of additives was measured and compared.

2.3. Characterization. The morphology of GABA crystals was characterized by optical polarizing microscopy (Olympus BX53, Japan). The particle size distribution was determined by a laser diffraction technique (Matersizer 3000, MalvernPanalytical, British). The crystal form was identified by powder X-ray diffraction (PXRD, Miniflex 600, Rigaku Corporation, Tokyo, Japan) using Cu Kα radiation (λ = 0.15405 nm). It was operated at 40 kV and 30 mA. The PXRD patterns were collected in a 2θ range from 5 to 50°, with a step size of 0.02° and a scanning speed of 8°·min^{-1}. The thermal analysis [thermogravimetric analysis (TGA)/differential scanning calorimetry (DSC)] of GABA was utilized to characterize the thermostability of GABA crystals using an integrated thermal analyzer (METTLER Toledo Instrument Co., Ltd.) under a nitrogen-purged atmosphere. The temperature started at 25 °C and ended at 300 °C at a heating rate of 10 °C·min^{-1}. Infrared (IR) spectra of GABA crystals were recorded with a Vertex 70 IR spectrometer (Germany). Measurements were made using KBr particles in the range of 4000−400 cm^{-1}, with a resolution of 4 cm^{-1}. Raman spectra were collected on a Raman spectrometer within the range 4000−0 cm^{-1}.

2.4. Molecular Simulation. The GABA crystal structure parameters used in the calculation are a = 7.193 Å, b = 10.120 Å, c = 8.260 Å, and Z = 4. It is monoclinic, and the space group is $P21c$.[24] In order to characterize the intermolecular interactions within GABA crystal, we performed Hirshfeld surface analysis and generated two-dimensional fingerprints with the CrystalExplorer 17.5 program, which accepted the structure input file in CIF format.[31] The crystal habit of GABA was predicted by the BFDH model in Materials Studio software.[32] The interaction between the GABA crystal surface and solvent was studied by molecular dynamics (MD) simulation. The effect of the additive was also explored via MD simulation. The COMPASS force field was used to distribute electric charge in the simulation.[33] The (100), (110), (010), and (001) faces were cut at a depth of 2 unit cells and subsequently extended to 3 × 4, 3 × 4, 4 × 3, and 4 × 4 supercell layers. A supersaturated solution system containing 200 water molecules and 50 GABA molecules was constructed using amorphous cell modules. For modeling additive systems, larger simulation box was needed, so we constructed HEC chains with 2 repeating units.[34] A solution layer without/with additive molecules was placed on the top of the crystal surface, and a vacuum plate with a thickness of 50 Å was added above the solution layer.[35]

Then, the energy minimization of the simulation box was carried out for the dynamic simulation. The van der Waals

https://doi.org/10.1021/acsomega.4c04625
ACS Omega 2024, 9, 29928−29938

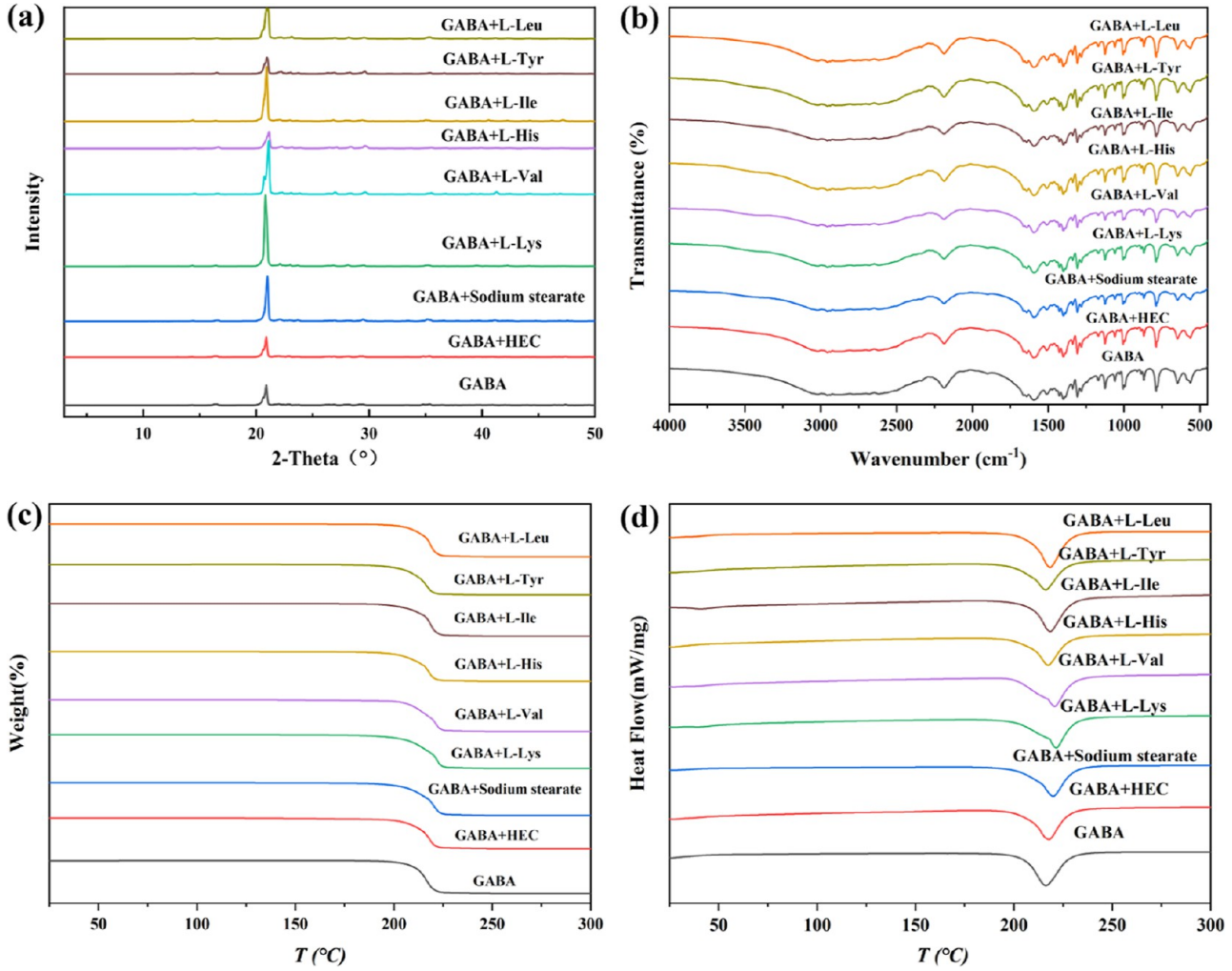

Figure 1. (a) PXRD pattern, (b) FTIR spectra, (c) TGA curves, and (d) DSC curves of GABA crystallized in the absence and presence of additives.

forces and electrostatic forces were calculated by using a group-based method, and the cutoff distance was set to 15.5 Å. MD simulation was performed in an *NVT* system with an Andersen thermostat at constant temperature (25 °C). The simulation was run at 500 ps with a time step of 1 fs, and the potential energy was calculated. In addition, the mean-square displacement (MSD) analysis was performed using simulated trajectories.[36] The interaction between the two components can be calculated as[37]

$$E_{AB} = E_{A+B} - (E_A + E_B) \quad (1)$$

where E_{A+B} is the total energy of the simulation box containing components A and B; E_A is the energy that component A removes from component B; and E_B is the energy of component B without component A.

3. RESULTS

3.1. Crystal Form Characterization. To investigate the effect of additives on the crystal form of GABA obtained during cooling crystallization, the solid samples were characterized by PXRD (Figure 1a). Comparing with the literature,[29] we found that GABA is the most stable form I in both raw materials and crystalline products obtained from cooling crystallization. In the absence or presence of additives, the PXRD peaks of GABA crystallization products were consistent with form I reported in the literature.[29,30] The additive did not change the crystal form of GABA particles.

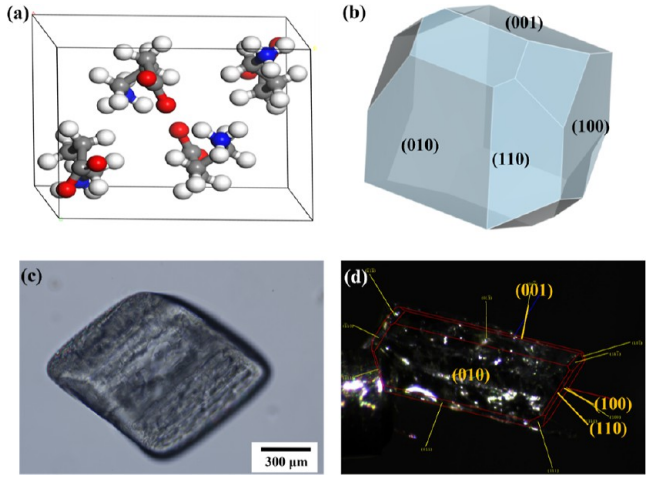

Figure 2. (a) Crystal structure of GABA, (b) crystal habit calculated by the BFDH model, (c) experimental crystal morphology in pure water, and (d) single crystal of GABA grown in the presence of additives with Miller indices of observable faces.

https://doi.org/10.1021/acsomega.4c04625
ACS Omega 2024, 9, 29928−29938

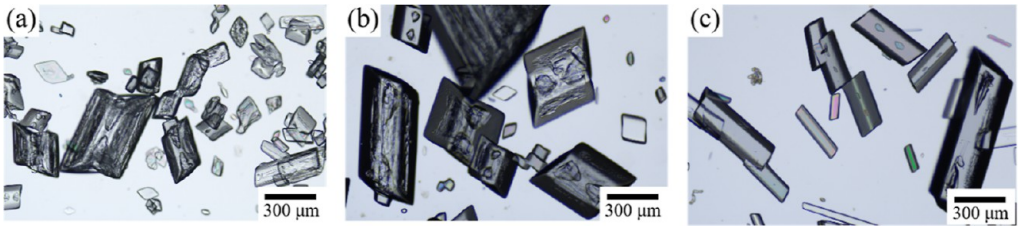

Figure 3. Optical micrographs of GABA crystals obtained at different HEC concentrations: (a) 0.005, (b) 0.01, and (c) 0.05%.

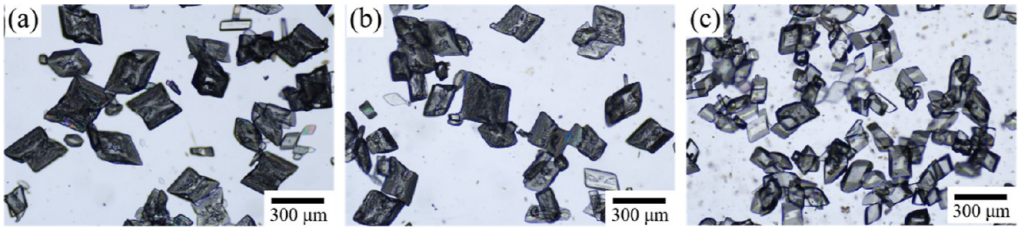

Figure 4. Microscopic images of GABA crystals prepared with different sodium stearate concentrations: (a) 0.005, (b) 0.01, and (c) 0.05%.

The peak strength of GABA crystals in the presence of different additives is different, which indicates that the morphology and particle size of GABA crystals change. Fourier transform infrared (FTIR) measurements showed no significant difference in the vibrational spectra of all GABA samples (Figure 1b). The Raman spectra of GABA crystals obtained with and without additives are also similar (Figure S2). These results indicated that there was no chemical structure change, and the additives were not incorporated into the crystal lattice. The thermal analysis of GABA (TGA/DSC) is shown in Figure 1c,d. Weight loss was observed when the temperature was heated to above 203 °C. Meanwhile, GABA crystals melted with decomposition. The TGA and DSC curves of samples obtained without and with additives are consistent, suggesting that there is no residue of solvent and additive. It also confirms the thermal stability of GABA during the crystallization process.[38]

3.2. Face Indexing. Based on the single-crystal structure of GABA extracted from the CCDC database (Figure 2a), the crystal morphology of GABA under a vacuum environment was predicted by the BFDH model. As shown in Figure 2b, the predicted crystal morphology is a polyhedral block. Cooling crystallization experiments were performed in pure water to investigate the crystal shape of GABA. The initial concentration, stirring rate, and cooling rate were screened. We found that under the saturated solution at 45 °C, the cooling rate of 0.2 min^{-1} was more conducive to GABA crystal growth. The crystal breakage degree was small when the stirring rate was 200 rpm. Plate-like crystals were grown from water (Figure 2c). Compared with the predicted habit, the relative surface area of different faces had changed in the experimental crystal shape. The single crystal in Figure 2d was prepared by slow evaporation of water in the presence of HEC. The length of GABA crystals grown in solution extended along the *a*-axis and was mainly related to the growth of (110) face and (100) face. The width increased toward the *c*-axis was related to the growth of the (001) face. Morphological important crystal face (010) along the *b*-axis affects the thickness of the crystal. Through the combination of experiment and simulation, (100) face, (110) face, (010) face, and (001) face were identified as the main crystal faces of GABA.

3.3. Effect of Additives on Crystal Morphology. *3.3.1. Polymer Additive.* Water-soluble polymer additives like polyvinylpyrrolidone, HEC, hydroxypropyl methyl cellulose, carboxymethyl cellulose, and methyl cellulose were studied. They are commonly used drug excipients and do not raise any regulatory issues in pharmaceutical crystallization.[39] We found that HEC had a significant effect on the crystal morphology of GABA in the cooling crystallization, and other polymer additives did not display a strong influence. With the increase of HEC concentration, obvious change of GABA crystal morphology could be observed (Figure 3). When the additive concentration was 0.005%, the crystal morphology was blocky. But the crystal surface was rough, exhibiting clear defects. With the increase of HEC concentration (0.05%), the growth of GABA crystal along the *a*-axis was enhanced, where the growth rate along the length being greater than that of other directions. The crystals exhibited a rod-like shape with a more smooth crystal surface.

3.3.2. Surfactant. Surfactant is a general term for compounds that can significantly reduce the surface tension of the solution.[40] In this work, surfactants were screened, and it was found that the crystal morphology of GABA was affected when sodium stearate was used as an additive (Figure 4). Block-like crystals were obtained with the presence of sodium stearate. As the additive concentration increased to 0.05%, crystal growth along the *a*-axis was clearly retarded. Meanwhile, crystals exhibited a smaller aspect ratio and smaller particle size.

3.3.3. Tailor-Made Additives. According to the molecular structure of GABA, six amino acids (L-Val, L-Leu, L-Ile, L-Lys, L-His, and L-Tyr) were used as tailor-made additives. The microscopic images of GABA obtained with various additives are shown in Figure 5. Besides active functional groups, L-Val is similar to GABA in carbon chain length. In the presence of L-Val, the crystal shape changed to an elongated plate-like shape when the additive concentration rose from 0.005 to 0.05%. The aspect ratio of crystals became apparently larger, and the thickness became thinner. Then, the effect of L-Leu and L-Ile was investigated, which have a longer carbon chain. In the presence of L-Leu, the grown crystals had a slightly larger aspect ratio, while block-like crystals were precipitated with L-Ile. The crystal morphology did not change greatly with the

https://doi.org/10.1021/acsomega.4c04625
ACS Omega 2024, 9, 29928−29938

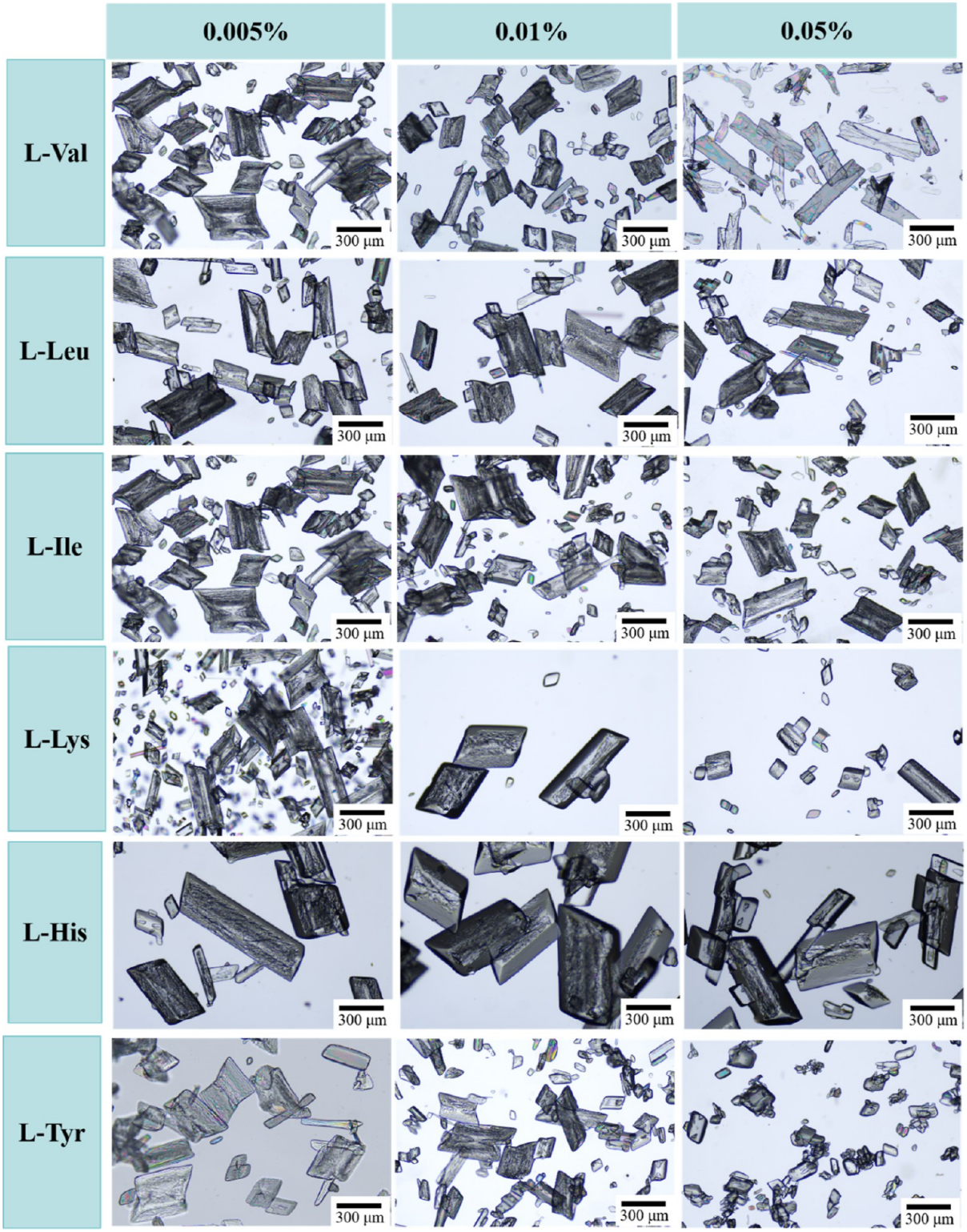

Figure 5. Microscopic images of GABA crystals prepared with tailor-made additives at different additive concentrations.

increase in the additive concentration. Tailor-made additive L-Lys was chosen because its carbon chain is longer, and there are two amino groups in the structure. When L-Lys was added into the aqueous solution, a mixture of block-like and rod-like crystals were obtained. Beside in addition to a carboxy group and an amino group, L-His also contains an imidazole group. In the presence of L-His, GABA crystals showed prismatic morphology and larger size. The additive concentration also showed little influence on crystal shape. Compared with GABA, L-Tyr contains an extra benzene ring and hydroxy group. Thinner plate-like crystals were grown in the presence of L-Tyr. Increased additive concentrations led to the formation of smaller particles. Therefore, tailor-made additives with similar structures and extra functional groups have interfered with the crystallization process. All of these amino

https://doi.org/10.1021/acsomega.4c04625
ACS Omega 2024, 9, 29928−29938

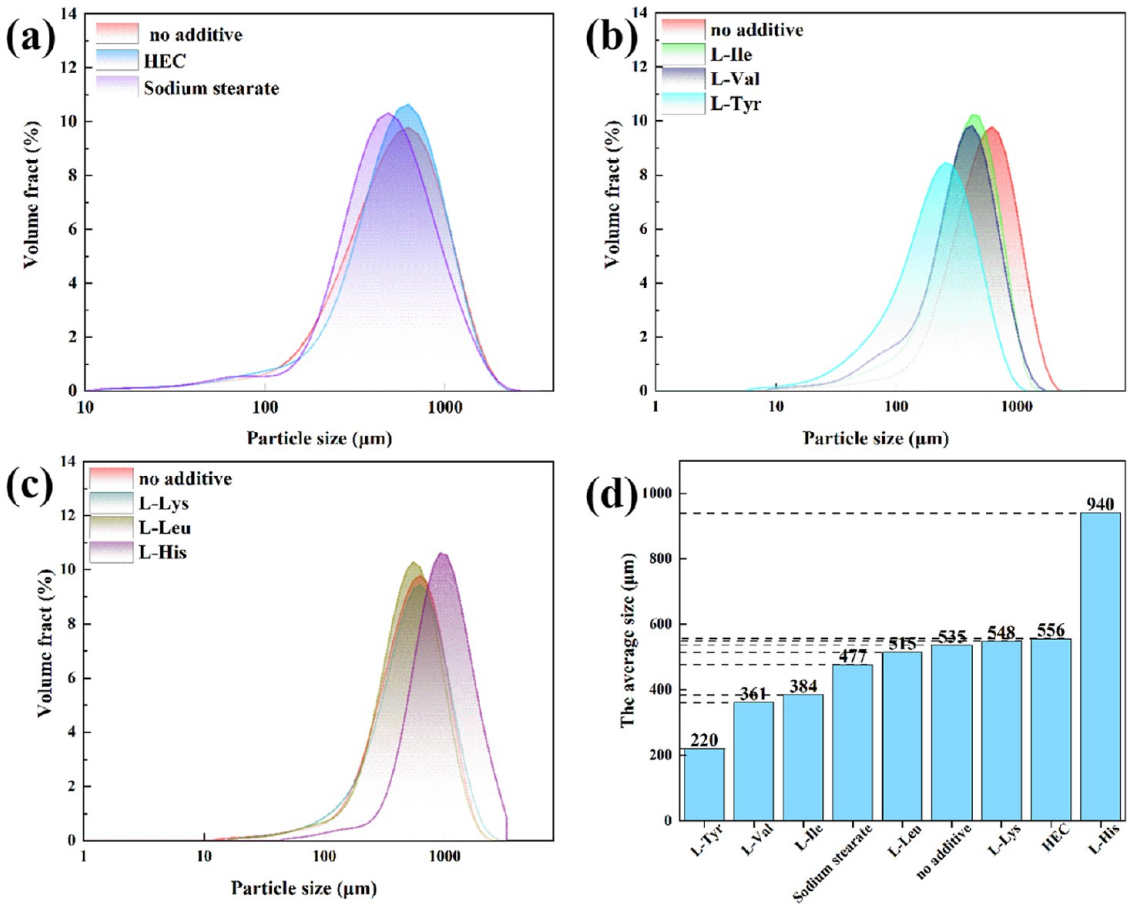

Figure 6. (a−c) Particle size distribution and (d) average size of GABA crystals prepared with different additives.

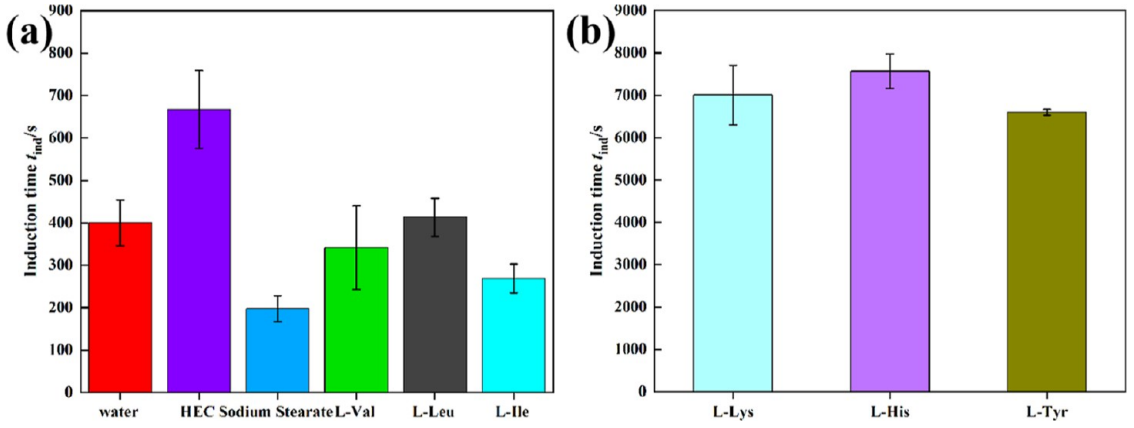

Figure 7. Induction time of GABA in pure water and in the presence of a 0.05% additive.

acids exhibited a certain influence on the crystal morphology of GABA.

The particle size distribution of GABA crystals was determined in the absence and presence of additives (0.05%). It can be seen from Figure 6 that sodium stearate reduced the particle size of GABA, while HEC slightly increased the particle size. For tailor-made additives, the addition of L-Tyr, L-Val and L-Ile decreased the particle size, L-Leu and L-Lys had little effect on crystal size, and L-His significantly increased the particle size of GABA. Among them, L-Tyr exhibited the strongest influence on reducing crystal size, where the average size decreased from 535 to 220 μm. In the presence of L-His, the average particle size increased greatly to 940 μm. Therefore, both the crystal shape and size can be modulated by additives.

3.4. Effect of Additives on Nucleation. During the cooling crystallization process, we found that the nucleation time of GABA was also affected by the additives. The induction time without/with 0.05% additives was measured under an initial supersaturation of 1.2 at 25 °C. The results are presented in Figure 7. In pure water, the induction time of GABA was about 400 s. When HEC was added to the solution, the induction time was extended to about 670 s, which displayed a nucleation inhibitory effect. Sodium stearate led to

https://doi.org/10.1021/acsomega.4c04625
ACS Omega 2024, 9, 29928−29938

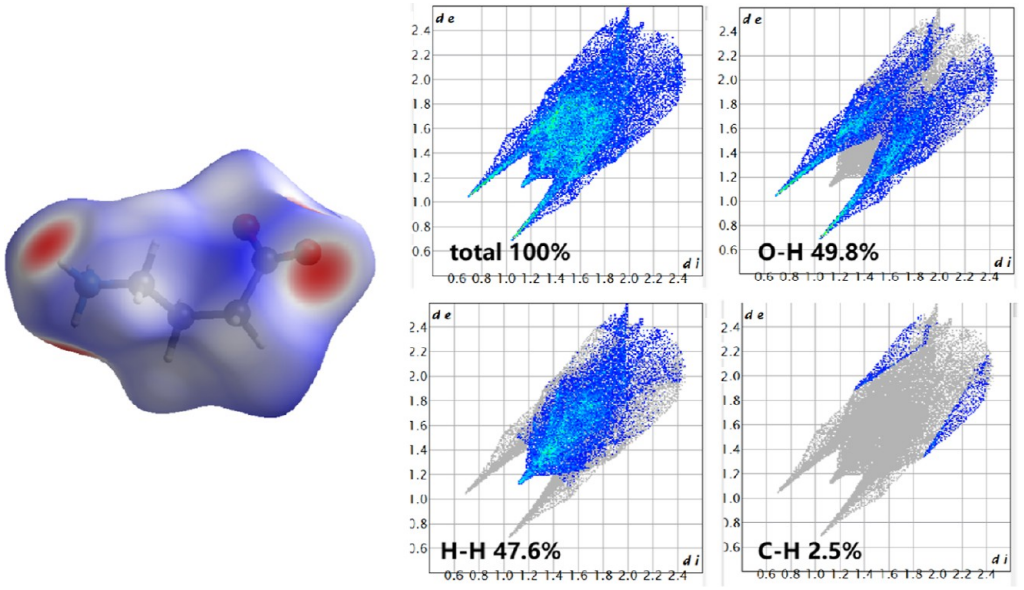

Figure 8. Hirshfeld surface mapped with d_{norm} and 2D fingerprint plots of GABA.

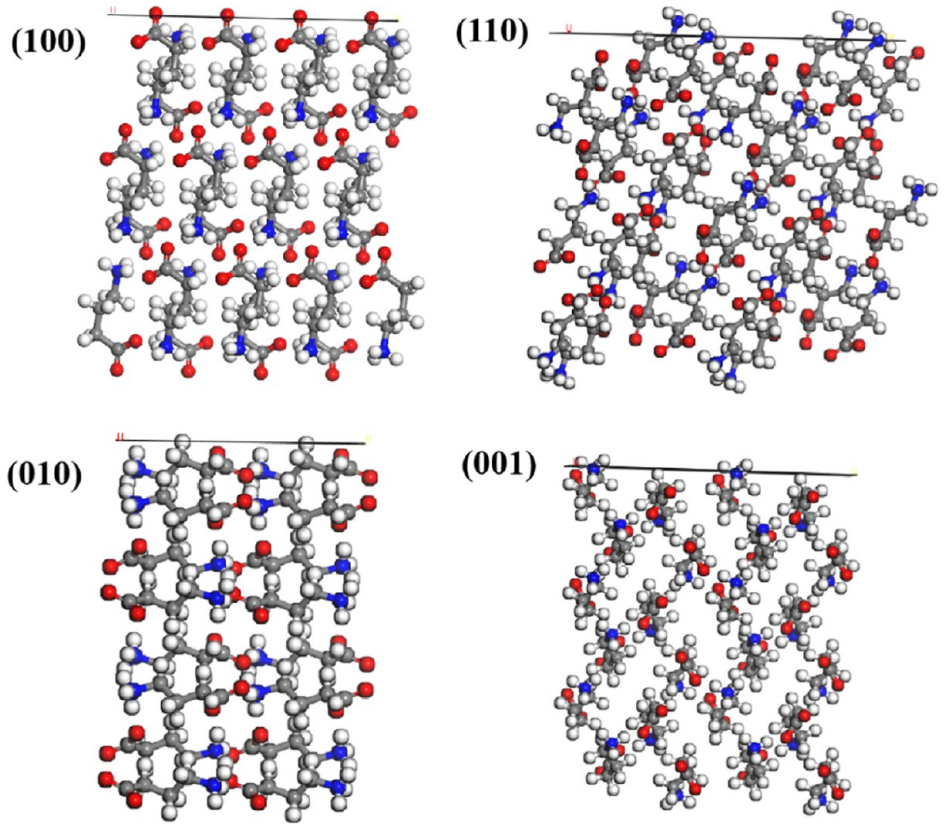

Figure 9. Surface structure of dominant crystal faces of GABA.

a shorter induction time of about 200 s, promoting nucleation of GABA. The amino acids L-Ile and L-Val slightly shortened the induction time, while L-Leu had negligible influence. Surprisingly, the presence of L-Lys, L-His, and L-Tyr significantly prolonged the induction time, which was more than 6500 s. Among all additives, L-His had the strongest inhibition of crystal nucleation.

3.5. Molecular Simulation and Analysis. *3.5.1. Surface Structure Analysis of GABA Crystal.* The Hirshfeld surface provides a three-dimensional image of close molecular contacts in the crystal, and these contacts can be summarized into a fingerprint plot.[31] The distances from a point on the Hirshfeld surface to the nearest nucleus inside and outside the surface can be defined as d_i and d_e, respectively. The normalized contact distance norm is defined in terms of d_e, d_i, and the van der Waals radius of the atom. The surface of Hirshfeld, drawn by d_{norm}, shows a red-white-blue color scheme, with contacts shorter than the van der Waals radius showing red spots. Using

https://doi.org/10.1021/acsomega.4c04625
ACS Omega 2024, 9, 29928−29938

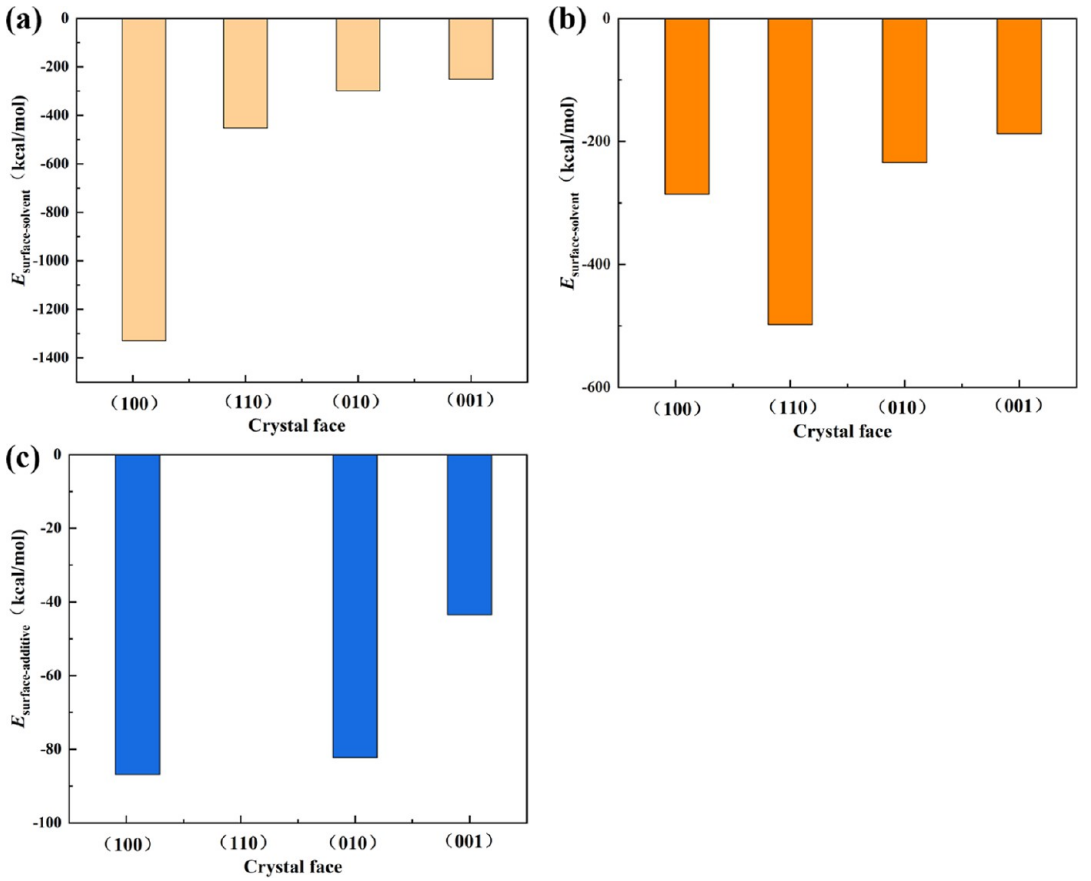

Figure 10. Interaction energies between the crystal surface and solvents in the (a) absence and (b) presence of additives. (c) Interaction energies between the crystal surface and additive.

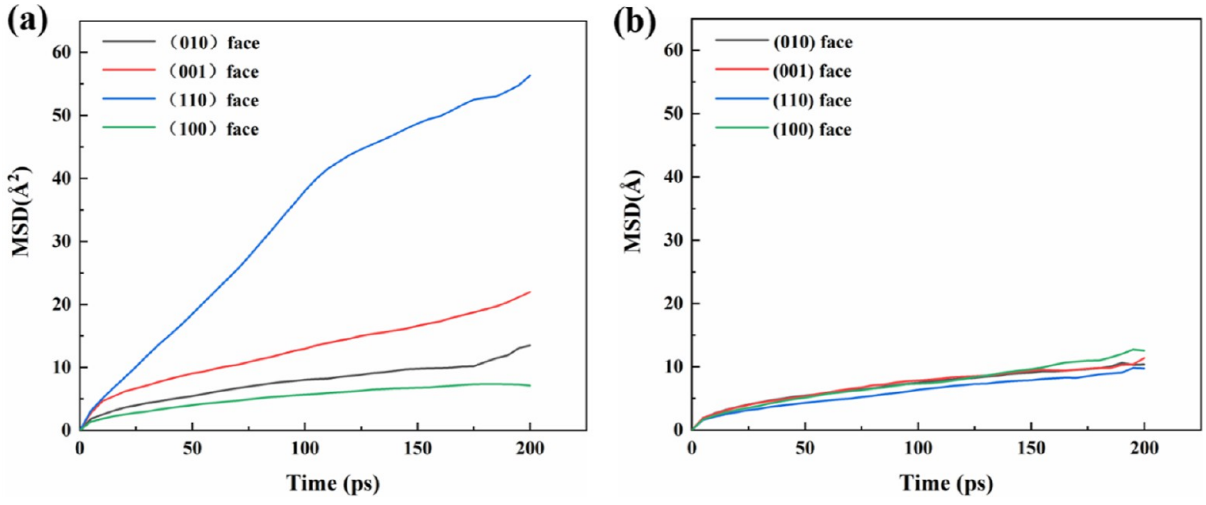

Figure 11. MSD of the solute molecules (a) in water and (b) in the presence of an additive.

these properties, we can also explore the types and proximity of intermolecular contacts in molecular crystals.[41] The Hirshfeld surface of GABA crystal was analyzed, and its norm surface is shown in Figure 8. Red spots on the surface indicate a close contact between the hydrogen bond donor and receptor. It can be seen that O...H contact contributes the most (49.8%). H...H intermolecular contacts account for 47.6% of the total surface area. The fingerprint plots exhibit a few C...H contacts, covering 2.5% of the surface area. It indicates that hydrogen bonding interactions may dominate the molecular interactions between GABA molecules.

The molecular topology of four important crystal faces (100), (110), (001), and (010) is shown in Figure 9. In the figure, gray balls represent carbon atoms, blue balls represent nitrogen atoms, red balls represent oxygen atoms, and white balls represent hydrogen atoms. On the (100) face, molecules array in parallel with each other, forming a flat surface. Both carboxyl groups and amino groups are all exposed, and carbonyl groups point out toward the surface. It enables the

https://doi.org/10.1021/acsomega.4c04625
ACS Omega 2024, 9, 29928−29938

approach of more GABA molecules and the formation of a hydrogen bond network. At the same time, it also allows for easy adsorption of water molecules. The chain of GABA molecules on the (110) face was tilted at a certain angle, and every two molecules are arranged in opposite directions. This surface is rough, and amino groups are exposed more prominently. On the (010) face, GABA molecules lie flat, displaying carboxyl groups, amino groups, and more methylene groups. Various functional groups are also displayed on the (001) surface. The GABA molecules in this face are arranged in a wave pattern.

3.5.2. MD Simulation. The aqueous solution−crystal systems of GABA in the absence and presence of additives were simulated, and the interaction force of the solvent−crystal surface was calculated. It can be seen from Figure 10a that the intermolecular interaction energy between (100) face and solvent is the strongest, followed by (110), (010), and (001) faces. This indicated that more water molecules are adsorbed on the surface of (100), and it will be more difficult for the solvent to desorb from the surface. Therefore, the growth of the (100) face was inhibited, resulting in a short plate-like shape.

Since HEC had the greatest impact on changing the crystal shape, it was selected to perform MD simulation. In the presence of HEC (Figure 10b), the interaction between the (100) face and solvent is significantly smaller, suggesting that the growth inhibition of this face by water is weakened. HEC had little influence on the interaction between solvent and the (110), (010), or (001) face. In addition, the interaction between the crystal face and additive is much smaller than that between the crystal face and solvent. There is also no interaction between the additive and (110) face. Under the effect of additive, the crystal growth along the *a*-axis will become faster, leading to rod-like shape.

We found that HEC also interacts with solute molecules in the solution, which may affect the self-assembly of GABA. The mobility of GABA molecules in crystal solution systems was explored in the absence and presence of HEC. The MSD of the solute in solution above different crystal faces was analyzed. It can be seen from Figure 11 that the MSD of solute in the system containing HEC was generally smaller than that in the system without additives. It indicates that additive molecules hinder the diffusion and migration of solute molecules. As a result, crystal nucleation was inhibited, which prolonged the induction period of GABA.

4. CONCLUSIONS

In this work, the effects of surfactants, polymer additives, and tailor-made additives on the crystal morphology of GABA were explored in cooling crystallization. In the presence of sodium stearate, smaller block-like crystals were obtained. Six kinds of amino acids were used as tailor-made additives, leading to the formation of plate-like, block-like, or prismatic crystals. L-His increased the particle size most significantly, and L-Tyr reduced the particle size most obviously. With increased concentration of HEC, the aspect ratio of crystals increased, and rod-like crystals were obtained. The induction time of GABA was determined without/with additives. The results indicated that sodium stearate promoted nucleation, while HEC, L-Lys, L-His, and L-Tyr inhibited nucleation. Hirshfeld surface analysis reveals dominant O...H and H...H contact interactions within the GABA crystal. Combined with crystal habit simulation and face indexing of single crystal, the (100), (110), (010), and (001) faces were identified as important crystal faces. To further study the effect of the additive, MD simulations were carried out establishing an aqueous solution−crystal system. The intermolecular forces between solvent and crystal surface in the absence and presence of HEC were calculated. In the presence of the additive, the molecular interaction between the (100) face and solvent becomes significantly smaller, indicating that the growth inhibition of water on the surface was weakened. The crystal growth along the *a*-axis would be accelerated, resulting in rod-like shape. The polymer additive also hindered the diffusion and migration of solute molecules and, thus, inhibited crystal nucleation. Therefore, effective additives have interfered with the crystallization process and play a crucial role in regulating the crystal shape and particle size.

■ ASSOCIATED CONTENT

Supporting Information

The Supporting Information is available free of charge at https://pubs.acs.org/doi/10.1021/acsomega.4c04625.

Chemical structure of additives (and Raman spectra of GABA obtained in the absence and presence of additives (PDF)

■ AUTHOR INFORMATION

Corresponding Authors

Yan Wang − *School of Pharmaceutical Sciences (Shandong Analysis and Test Center), Qilu University of Technology (Shandong Academy of Sciences), Jinan 250014, P. R. China*; Email: wangyan57@qlu.edu.cn

Shichao Du − *School of Pharmaceutical Sciences (Shandong Analysis and Test Center), Qilu University of Technology (Shandong Academy of Sciences), Jinan 250014, P. R. China*; orcid.org/0000-0002-8369-2983; Email: shichao_du@qlu.edu.cn

Fumin Xue − *School of Pharmaceutical Sciences (Shandong Analysis and Test Center), Qilu University of Technology (Shandong Academy of Sciences), Jinan 250014, P. R. China*; Email: xuefumin@qlu.edu.cn

Authors

Zhiying Pan − *School of Pharmaceutical Sciences (Shandong Analysis and Test Center), Qilu University of Technology (Shandong Academy of Sciences), Jinan 250014, P. R. China*

Xiaoyu Cao − *School of Pharmaceutical Sciences (Shandong Analysis and Test Center), Qilu University of Technology (Shandong Academy of Sciences), Jinan 250014, P. R. China*

Wenyu Ke − *School of Pharmaceutical Sciences (Shandong Analysis and Test Center), Qilu University of Technology (Shandong Academy of Sciences), Jinan 250014, P. R. China*

Jingyu Wang − *School of Pharmaceutical Sciences (Shandong Analysis and Test Center), Qilu University of Technology (Shandong Academy of Sciences), Jinan 250014, P. R. China*

Complete contact information is available at: https://pubs.acs.org/10.1021/acsomega.4c04625

Notes

The authors declare no competing financial interest.

■ ACKNOWLEDGMENTS

The authors are grateful to the financial support by the National Natural Science Foundation of China (22378216 and

22008175), the Key R&D Program of Shandong Province (2021CXGC010514), the Youth Innovation Team of Universities in Shandong Province (2023KJ141), the Talent Research Project of Qilu University of Technology (2023RCKY076), and the Jinan Introducing Innovation Team Project (202228033).

REFERENCES

(1) Addadi, L.; Berkovitch-Yellin, Z.; Weissbuch, I.; van Mil, J.; Shimon, L. J. W.; Lahav, M.; Leiserowitz, L. Growth and Dissolution of Organic Crystals with "Tailor-Made" Inhibitors—Implications in Stereochemistry and Materials Science. *Angew. Chem., Int. Ed.* **1985**, *24* (6), 466−485.

(2) Nagy, Z. K.; Fevotte, G.; Kramer, H.; Simon, L. L. Recent advances in the monitoring, modelling and control of crystallization systems. *Chem. Eng. Res. Des.* **2013**, *91* (10), 1903−1922.

(3) Kim, K.-J. Industrial Crystallization. *Chem. Eng. Technol.* **2016**, *39* (7), 1212.

(4) Han, B.; Bockman, O.; Wilson, B. P.; Lundström, M.; Louhi-Kultanen, M. Purification of Nickel Sulfate by Batch Cooling Crystallization. *Chem. Eng. Technol.* **2019**, *42* (7), 1475−1480.

(5) Nagy, B.; Szilágyi, B.; Domokos, A.; Tacsi, K.; Pataki, H.; Marosi, G.; Nagy, Z. K.; Nagy, Z. K. Modeling of pharmaceutical filtration and continuous integrated crystallization-filtration processes. *Chem. Eng. J.* **2021**, *413*, 127566.

(6) Yu, S.; Wang, Z.; Ma, Y.; Xue, F. Effect of natural polymer additives on crystal form and morphology of clozapine anhydrate and monohydrate. *J. Mol. Liq.* **2022**, *364*, 119985.

(7) Wang, Y.; Zhang, H.; Cai, L.; Xue, F.; Chen, H.; Gong, J.; Du, S. Polymer-mediated and ultrasound-assisted crystallization of ropivacaine: Crystal growth and morphology modulation. *Ultrason. Sonochem.* **2023**, *97*, 106475.

(8) Liu, Q.; Wang, J.; Wu, H.; Zong, S.; Huang, X.; Wang, T.; Hao, H. Manipulating of Crystal Morphology and Polymorph by Crystallization in Microemulsions. *Ind. Eng. Chem. Res.* **2020**, *59* (29), 13024−13032.

(9) Bötschi, S.; Rajagopalan, A. K.; Rombaut, I.; Morari, M.; Mazzotti, M. From needle-like toward equant particles: A controlled crystal shape engineering pathway. *Comput. Chem. Eng.* **2019**, *131*, 106581.

(10) Phan, C. U.; Shen, J.; Yu, K.; Mao, J.; Tang, G. Impact of Crystal Habit on the Dissolution Rate and In Vivo Pharmacokinetics of Sorafenib Tosylate. *Molecules* **2021**, *26* (11), 3469.

(11) Berry, J.; Kline, L. C.; Sherwood, J. K.; Chaudhry, S.; Obenauer-Kutner, L.; Hart, J. L.; Sequeira, J. Influence of the Size of Micronized Active Pharmaceutical Ingredient on the Aerodynamic Particle Size and Stability of a Metered Dose Inhaler. *Drug Dev. Ind. Pharm.* **2004**, *30* (7), 705−714.

(12) Yuan, P. Q.; Liu, B. S.; Sun, H. Optimization of the Crystallization Process of Bis(2-hydroxyethyl) Terephthalate. *Cryst. Res. Technol.* **2021**, *56* (11), 2100025.

(13) Feng, Y.; Chen, S.; Li, Z.; Gu, Z.; Xu, S.; Ban, X.; Hong, Y.; Cheng, L.; Li, C. A review of controlled release from cyclodextrins: release methods, release systems and application. *Crit. Rev. Food Sci. Nutr.* **2023**, *63* (20), 4744−4756.

(14) Ren, Y.; Shen, J.; Yu, K.; Phan, C. U.; Chen, G.; Liu, J.; Hu, X.; Feng, J. Impact of Crystal Habit on Solubility of Ticagrelor. *Crystals* **2019**, *9* (11), 556.

(15) Thorat, A. A.; Dalvi, S. V. Ultrasound-assisted modulation of concomitant polymorphism of curcumin during liquid antisolvent precipitation. *Ultrason. Sonochem.* **2016**, *30*, 35−43.

(16) Civati, F.; Svoboda, V.; Urwin, S. J.; McArdle, P.; Erxleben, A.; Croker, D.; ter Horst, J. Manipulating Cocrystal Size and Morphology using a Combination of Temperature Cycling and Additives. *Cryst. Growth Des.* **2021**, *21* (3), 1496−1506.

(17) Li, Z.; Shi, P.; Yang, Y.; Sun, P.; Wang, Y.; Xu, S.; Gong, J. Tuning crystallization and stability of the metastable polymorph of dl-methionine by a structurally similar additive. *CrystEngComm* **2019**, *21* (24), 3731−3739.

(18) Kim, I. W.; Robertson, R. E.; Zand, R. Effects of Some Nonionic Polymeric Additives on the Crystallization of Calcium Carbonate. *Cryst. Growth Des.* **2005**, *5* (2), 513−522.

(19) Xie, S.; Poornachary, S. K.; Chow, P. S.; Tan, R. B. H. Direct Precipitation of Micron-Size Salbutamol Sulfate: New Insights into the Action of Surfactants and Polymeric Additives. *Cryst. Growth Des.* **2010**, *10* (8), 3363−3371.

(20) Mojibola, A.; Dongmo-Momo, G.; Mohammed, M.; Aslan, K. Crystal Engineering of l-Alanine with l-Leucine Additive using Metal-Assisted and Microwave-Accelerated Evaporative Crystallization. *Cryst. Growth Des.* **2014**, *14* (5), 2494−2501.

(21) Poornachary, S. K.; Chow, P. S.; Tan, R. B. H. Effect of solution speciation of impurities on α-glycine crystal habit: A molecular modeling study. *J. Cryst. Growth* **2008**, *310* (12), 3034−3041.

(22) Xu, S. J.; Cao, D.; Liu, Y. X.; Wang, Y. F. Role of Additives in Crystal Nucleation from Solutions: A Review. *Cryst. Growth Des.* **2022**, *22* (3), 2001−2022.

(23) Rashmi, D.; Zanan, R.; John, S.; Khandagale, K.; Nadaf, A. γ-Aminobutyric Acid (GABA): Biosynthesis, Role, Commercial Production, and Applications. *Stud. Nat. Prod. Chem.* **2018**, *57*, 413−452.

(24) Tomita, K.-i.; Higashi, H.; Fujiwara, T. Crystal and Molecular Structure of ω-Amino Acids, ω-Amino Sulfonic Acids and Their Derivatives. IV. The Crystal and Molecular Structure of γ-Aminobutyric Acid (GABA), a Nervous Inhibitory Transmitter. *Bull. Chem. Soc. Jpn.* **1973**, *46* (7), 2199−2204.

(25) Li, K.; Xu, E. The role and the mechanism of γ-aminobutyric acid during central nervous system development. *Neurosci. Bull.* **2008**, *24* (3), 195−200.

(26) Diana, M.; Quílez, J.; Rafecas, M. Gamma-aminobutyric acid as a bioactive compound in foods: a review. *J. Funct.* **2014**, *10*, 407−420.

(27) Zhao, K.; Yang, P.; Du, S.; Li, K.; Li, X.; Li, Z.; Liu, Y.; Lin, L.; Hou, B.; Gong, J. Determination and correlation of solubility and thermodynamics of mixing of 4-aminobutyric acid in mono-solvents and binary solvent mixtures. *J. Chem. Thermodyn.* **2016**, *102*, 276−286.

(28) Dobson, A. J.; Gerkin, R. E. γ-Aminobutyric Acid: a Novel Tetragonal Phase. *Acta Crystallogr., Sect. C: Cryst. Struct. Commun.* **1996**, *52* (12), 3075−3078.

(29) Wang, L.; Tang, W.; Du, S.; Xu, S.; Shi, P.; Wu, S.; Gong, J. Surprising Effect of Carbon Chain Length on Inducing Ability of Additives: Elusive Form-II of γ-Aminobutyric Acid (GABA) Induced by Sodium Carboxylate Additives. *Cryst. Growth Des.* **2019**, *19* (7), 3825−3833.

(30) Wang, L.; Sun, G.; Zhang, K.; Yao, M.; Jin, Y.; Zhang, P.; Wu, S.; Gong, J. Green Mechanochemical Strategy for the Discovery and Selective Preparation of Polymorphs of Active Pharmaceutical Ingredient γ-Aminobutyric Acid (GABA). *ACS Sustainable Chem. Eng.* **2020**, *8* (45), 16781−16790.

(31) Spackman, M. A.; Jayatilaka, D. Hirshfeld surface analysis. *CrystEngComm* **2009**, *11* (1), 19−32.

(32) Du, S.; Yu, C.; Zhang, P.; Lu, J.; Gong, J.; Xue, F.; Wang, Y. Hierarchical Structure of Glucosamine Hydrochloride Crystals in Antisolvent Crystallization. *Crystals* **2023**, *13* (9), 1307.

(33) Li, D.; Cai, J.; Guo, B.; Wei, D.; Liu, Q.; Liu, B. Controllable crystallization of urea crystal face (0 0 1) by molecular simulation. *J. Cryst. Growth* **2019**, *524*, 125139.

(34) Liu, F.; Wang, L.; Li, W.; Li, M.; Gong, J.; Wang, Y.; Han, D. Crystal Growth of l-Alanine with Glycine-Based Oligopeptides: The Revelation for the Competitive Mechanism. *Cryst. Growth Des.* **2021**, *21* (7), 3818−3830.

(35) Shim, H.-M.; Myerson, A. S.; Koo, K.-K. Molecular Modeling on the Role of Local Concentration in the Crystallization of l-Methionine from Aqueous Solution. *Cryst. Growth Des.* **2016**, *16* (6), 3454−3464.

(36) Zhang, S. H.; Zhou, L.; Yang, W. C.; Xie, C.; Wang, Z.; Hou, B. H.; Hao, H. X.; Zhou, L. N.; Bao, Y.; Yin, Q. X. An Investigation into

https://doi.org/10.1021/acsomega.4c04625
ACS Omega 2024, 9, 29928−29938

the Morphology Evolution of Ethyl Vanillin with the Presence of a Polymer Additive. *Cryst. Growth Des.* **2020**, *20* (3), 1609−1617.
(37) Wang, Y.; Xue, F.; Yu, S.; Cheng, Y.; Yin, M.; Du, S.; Gong, J. Insight into the morphology and crystal growth of DL-methionine in aqueous solution with presence of cellulose polymers. *J. Mol. Liq.* **2021**, *343*, 116967.
(38) Zhao, K.; Lin, L.; Li, C.; Du, S.; Huang, C.; Qin, Y.; Yang, P.; Li, K.; Gong, J. Measurement and Correlation of Solubility of γ-Aminobutyric Acid in Different Binary Solvents. *J. Chem. Eng. Data* **2016**, *61* (3), 1210−1220.
(39) Bellucci, M. A.; Marx, A.; Wang, B.; Fang, L.; Zhou, Y.; Greenwell, C.; Li, Z.; Becker, A.; Sun, G.; Brandenburg, J. G.; Sekharan, S. Effect of Polymer Additives on the Crystal Habit of Metformin HCl. *Small Methods* **2023**, *7* (6), 2201692.
(40) Shaban, S. M.; Kang, J.; Kim, D.-H. Surfactants: Recent advances and their applications. *Compos. Commun.* **2020**, *22*, 100537.
(41) Sundareswaran, S.; Karuppannan, S. Hirshfeld Surface Analysis of Stable and Metastable Polymorphs of Vanillin. *Cryst. Res. Technol.* **2020**, *55* (11), 2000083.

https://doi.org/10.1021/acsomega.4c04625
ACS Omega 2024, 9, 29928−29938